NOTES AND CORRESPONDENCE

Measuring Surface Currents in Drake Passage from Altimetry and Hydrography

P. G. CHALLENOR

James Rennell Division for Ocean Circulation, Southampton Oceanography Centre, Southampton, United Kingdom

J. F. READ AND R. T. POLLARD

George Deacon Division for Ocean Processes, Southampton Oceanography Centre, Southampton, United Kingdom

R. T. TOKMAKIAN

Naval Postgraduate School, Monterey, California

4 April 1995 and 10 April 1996

ABSTRACT

This paper describes a new method for combining altimetry data with hydrography in order to produce absolute surface geostrophic currents from altimetry. This method is then applied to data from the Drake Passage allowing surface currents to be monitored every 35 days during the second half of 1992. The resulting currents show several regions of strong currents with water flowing to the east and other places where the currents are either zero or flowing to the west. After comparison with a model it is suggested that this structure is a result of the bathymetry.

1. Introduction

Radar altimeters have proved to be formidable weapons in the oceanographers' armory. However, because we do not know the shape of the geoid to sufficient accuracy, it is impossible to derive mean currents on scales less than about 2000 km, where the geoid models are thought to be good, from altimetry alone, and almost all altimeter studies on smaller scales have concentrated on the variability of currents. A number of proposals have been made to launch satellites specifically to measure the earth's gravity field and hence the geoid (Gleason 1991; Jekeli and Upadhyay 1990; Lambeck 1990). So far none of these missions has been approved, although some are still pending. In the absence of accurate measurements of the geoid at high wavenumbers we must either be satisfied with only measuring variability or we must use special techniques to get around the problem. A number of attempts have been made to use "synthetic" geoids (Kelly and Gille 1990; Glenn et al. 1991) derived from modeling the mean current in some way. This paper describes a new method that enables mean currents to be derived using a combination of altimeter and in situ observations and makes no assumptions about the structure of the mean current. Similar methods have been suggested before (Ozimek et al. 1993; Mitchell et al. 1990), but the quality of the available data in the past was not good enough to allow the results to be fully exploited.

The theoretical basis of the method is described in section 2. Section 3 contains a discussion of the practical problems encountered in applying the new method. The technique is then applied to an *ERS-1* track across the Drake Passage (section 4). After a discussion of the ship data the results of applying the method are given. This is followed by a comparison with a high-resolution global model. Section 5 contains our conclusions.

2. Theory

Although it is possible to justify the method by statistical arguments, it is instructive to derive it from dynamical considerations. Let the height of the sea surface relative to the reference ellipsoid (as measured by the altimeter, assuming perfect corrections) be h.

Let the height of the sea surface relative to a true level of no motion be H. Since the geoid is parallel to a level of no motion, the height of the geoid relative to the ellipsoid is given by

$$G \pm k = H_{t_0} - h_{t_0}, \tag{1}$$

Corresponding author address: Peter G. Challenor, James Rennell Division for Ocean Circulation, Southampton Oceanography Centre, Empress Dock, Southampton SO14 3ZH, United Kingdom.

© 1996 American Meteorological Society

Unauthenticated | Downloaded 01/22/22 03:01 AM UTC

where k is an unknown constant and the subscript gives the time at which the measurements were taken.

Differentiating w.r.t. x (the direction along which the measurements are taken)

$$\frac{\partial G}{\partial x} = \frac{\partial H_{t_0}}{\partial x} - \frac{\partial h_{t_0}}{\partial x}. \quad (2)$$

Since G is invariant with time,

$$\frac{\partial H_t}{\partial x} = \frac{\partial H_{t_0}}{\partial x} - \left(\frac{\partial h_{t_0}}{\partial x} - \frac{\partial h_t}{\partial x}\right). \quad (3)$$

Thus, we can calculate the alongtrack slope of the sea surface relative to the geoid at time t from the altimeter measurement of surface height if we have simultaneous measurements of the sea surface height relative to a level of no motion and the altimeter.

From geostrophy

$$\frac{\partial H_t}{\partial x} = \frac{f v_t}{g}, \quad (4)$$

where v_t is the geostrophic current, f is the Coriolis parameter, and g is the acceleration due to gravity:

$$\therefore v_t = v_{t_0} - \frac{g}{f}\left(\frac{\partial h_{t_0}}{\partial x} - \frac{\partial h_t}{\partial x}\right). \quad (5)$$

Therefore, if we measure the surface geostrophic current simultaneously with an altimeter pass, we can estimate the surface current at any time the altimeter takes a measurement along the same track.

3. Practical considerations

In deriving the above relationship a number of assumptions have been made. Most of these have to do with the altimeter measurements. It has been assumed that we have been able to derive an error-free estimate of the height of the sea surface above a reference ellipsoid. In practice this is impossible to achieve. In addition to the inherent inaccuracy in any measurement there are a number of corrections that need to be made to the altimeter measurement, which are often imperfectly known. The major uncertainty at the present time is the radial orbit. The altimeter measures the position of the satellite relative to the sea surface, while an orbit prediction is used to calculate the position of the satellite relative to the ellipsoid. The orbit error in particular, but also some of the other corrections, vary on much larger scales than the currents we are trying to measure. Thus, the errors can be approximated over small scales by a linear function; that is,

$$h' = \alpha + \beta x + h.$$

Differentiating to produce slopes,

$$\frac{\partial h'}{\partial x} = \beta + \frac{\partial h}{\partial x}.$$

Thus, any error that is on such a large scale as to be represented by a bias term is removed when we calculate the slopes, whereas any shorter-scale error that is approximated by a tilt will become a bias. We do not need to worry, therefore, about corrections (or errors in corrections) that are on much larger scales than the section being considered.

It has also been assumed that we can measure the surface geostrophic current at time t_0. As is well known, the interior of the ocean can be assumed to be in geostrophic balance, but currents at the surface have a large ageostrophic component. We cannot therefore measure the surface geostrophic current directly. The method we have used in this paper is described in detail below but in essence is as follows: We have ADCP measurements of the true current (geostrophic + ageostrophic) and measurements of density from a CTD. These density measurements can be used to evaluate a geostrophic shear between the surface and some depth (say 200–300 m), but we need to add an estimate of the geostrophic current at that depth to infer the absolute surface geostrophic current. We obtain that estimate by assuming that the ADCP is measuring the geostrophic current at depth.

4. Monitoring the flow through the Drake Passage

In November 1992 RRS *Discovery* sailed from the Falkland Islands to Elephant Island across Drake Pas-

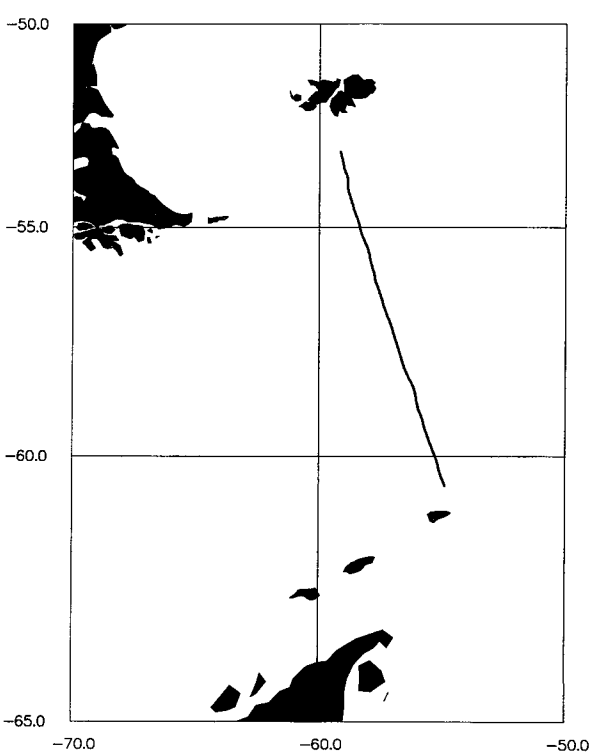

FIG. 1. Cruise track.

Unauthenticated | Downloaded 01/22/22 03:01 AM UTC

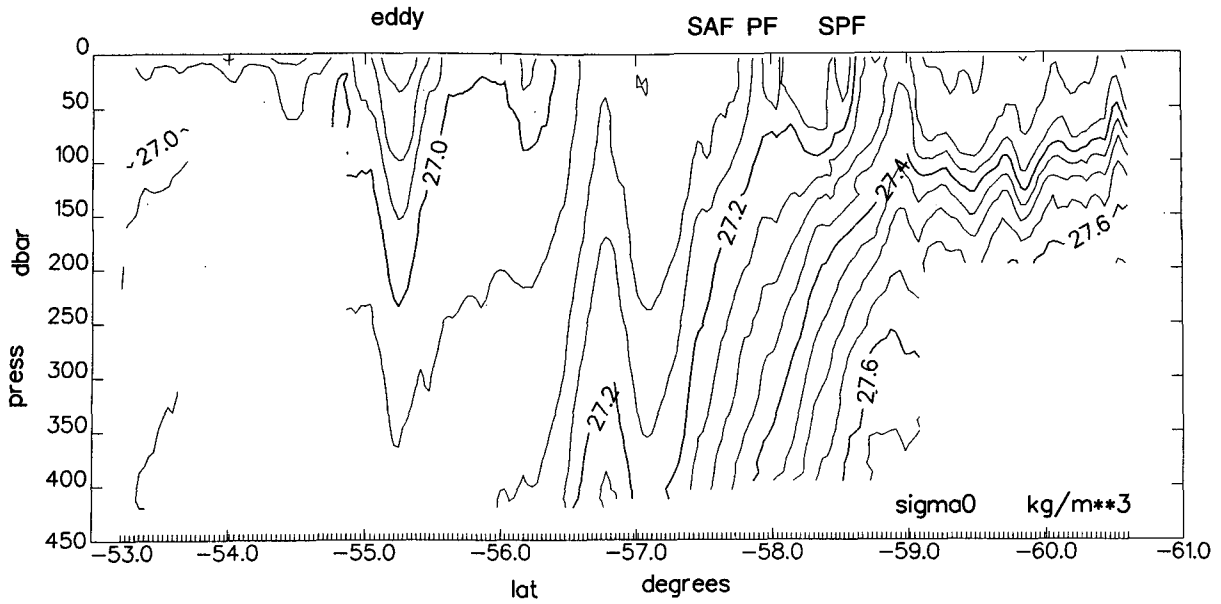

FIG. 2. SeaSoar CTD-derived density (calculated relative to the surface) down to 400 m across Drake Passage from Burdwood Bank to just north of Elephant Island. The lack of deep data at the southern end of the section was the result of thick and patchy fog and the risk of icebergs. The SeaSoar had to be towed on a shortened cable, so it could not reach its full depth. The positions of the major fronts are marked (SAF, Subantarctic Front; PF, Polar Front; SPF, Southern Polar Front). Note the eddy at 55.2°S and an apparent eddy just north of the SAF at 56.8°S.

sage as part of the Sterna 92 cruise (Turner 1993) (Fig. 1). The line followed is WOCE line SR1 and lies along an *ERS-1* ascending track in the 35-day repeat part of the mission. *ERS-1* collected data along this track on day 314 of 1992. The ship moved south along the track from day 315 to 317. *Discovery* towed an undulating SeaSoar carrying a CTD and an Acoustic Doppler Current Profiler (ADCP). This was the first trial of the ASTECH GPS system for obtaining the ship's heading for correcting the gyro error in the ADCP measurement (Griffiths 1994; King and Cooper 1994).

ERS-1 traverses this pass every 35 days and good data are available from days 139, 174, 209, 244, 279, 314, and 349 of 1992 and days 18, 158, 193, and 263 of 1993. *ERS-1* stayed in this orbit from April 1992 to the end of 1993 and both *ERS-1* and *ERS-2* should be in the same orbit again at the beginning of 1995. Thus, using the method proposed here, it is possible to monitor the flow through this part of the Drake Passage for 18 months with *ERS-1* data and for 3–5 years with *ERS-2,* which is expected to stay in the same orbit for its entire operational lifetime.

a. Results from the Sterna 92 cruise

Temperature and salinity data were collected from the top 400 m of the water column using SeaSoar, while *Discovery* steamed south along the *ERS-1* track at 8 knots (15 m s^{-1}) (Read et al. 1993; Turner 1993). SeaSoar is a towed undulating vehicle carrying a Neil Brown Instrument System Mark 3 CTD. It cycles through the water column from the surface to 400 m and back approximately once every 15 minutes (Pollard 1986). Temperature and pressure were calibrated from precruise laboratory calibrations, and salinity was calibrated from underway salinity samples drawn from the nontoxic pumped supply. To check variations of salinity with depth, the resultant $\theta-S$ profiles were compared with those from a cruise two months earlier (R. Peterson 1995, personal communication), which partly followed the same WOCE line. No bias could be detected (Read et al. 1993).

In order to minimize the effects of internal waves, the data were smoothed by averaging over 12 km onto a 4-km horizontal grid with 8-dbar spacing vertically. A few gaps of missing data were linearly interpolated. Density (sigma0) was calculated relative to the surface (Fig. 2), and geostrophic shear (Fig. 3) was then calculated between adjacent columns of the 4-km grid. Because of the 12-km averaging, adjacent columns are not independent, and the effect of differencing 12-km averages 4 km apart in the geostrophic calculation is exactly equivalent to differencing independent 4-km averages 12 km apart (Pollard et al. 1987). The 4-km averaging reduces the noise caused by short wavelength, short-period internal waves. The 12-km differencing of data collected within an hour minimizes errors that would be introduced by long-period internal waves (tides and inertial oscillations) while resolving mesoscale structure.

Unauthenticated | Downloaded 01/22/22 03:01 AM UTC

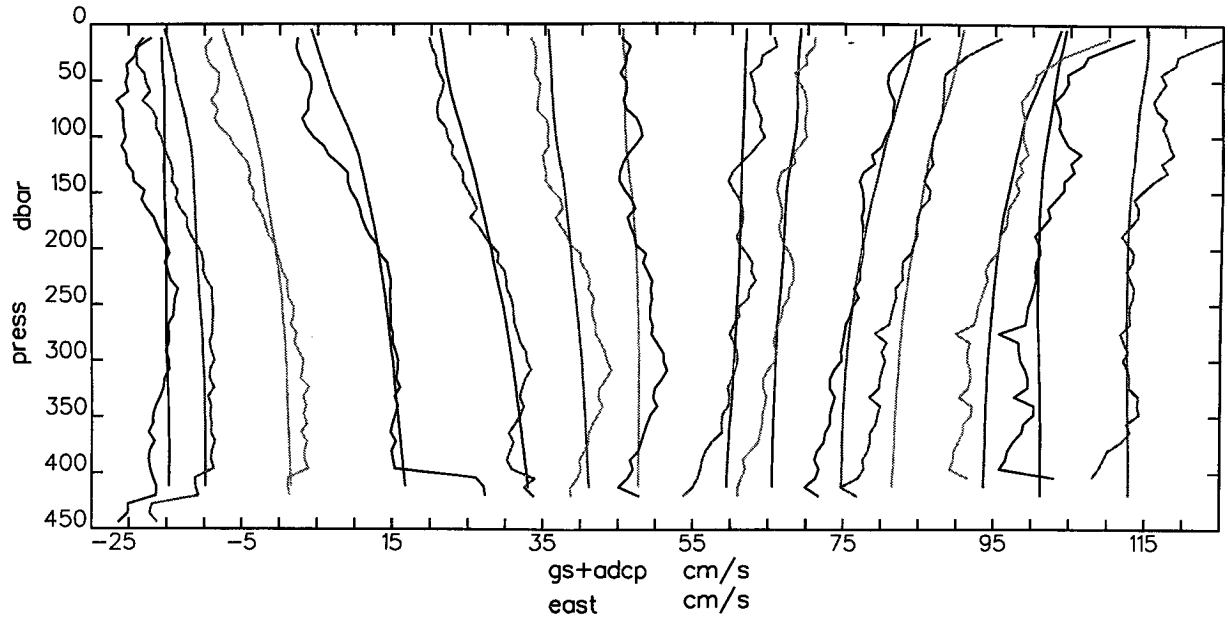

FIG. 3. Profiles of the component of ADCP velocity perpendicular to the ship's track (jagged) and the geostrophic shear (smooth) are shown for a series of profiles across the eddy between 54.02° and 55.46°S (Fig. 2). Both ADCP and SeaSoar density profiles were averaged over 12 km into 4-km intervals. Geostrophic velocity was calculated between 4-km pairs of density profiles. The scale on the x axis refers to the first ADCP profile. Each subsequent ADCP profile is offset by 5 cm s^{-1}. The geostrophic shear profiles are adjusted to match the corresponding ADCP profile at 196 m.

Velocity data were collected in 2-minute ensembles from an RD Instruments ship-mounted Acoustic Doppler Current Profiler. The data were calibrated for misalignment angle and speed (Pollard and Read 1989) and averaged over 15 minutes to form approximately 4-km averages. The cruise was the first full scientific cruise on which *Discovery* was fitted with an ASHTECH 3D-GPS set (Griffiths 1994; King and Cooper 1993), which measured the heading more accurately than can be achieved with normal ship's gyro. Thus, ASHTECH heading rather than gyro heading was used in the calculation of the misalignment angle; details are given in Griffiths (1994). The estimated errors in the absolute ADCP velocity, averaged over 12 minutes was 0.05 m s^{-1}. Corrected ADCP current vectors at 196-m depth are shown in Fig. 4.

We seek to use the SeaSoar and ADCP data to derive surface geostrophic velocity. The SeaSoar data alone are inadequate as they do not extend deep enough, and the geostrophic velocities a few hundred meters deep are large. Near-surface ADCP velocities may be significantly ageostrophic because of wind-driven Ekman transport and inertial oscillations, and ADCP velocities at all depths will be contaminated by internal waves and tides. Our solution is to combine the geostrophic shear with the ADCP cross-track velocity at a depth well below the mixed layer. This assumes that wind-driven motions are small below the mixed layer so that the ADCP velocities are nearly geostrophic. We spatially average the ADCP velocities to reduce internal wave noise.

Matched ADCP velocities to geostrophic shear profiles was used successfully by Pollard and Regier (1992), but their two-dimensional survey allowed a streamfunction to be fitted to both components of the ADCP velocity vectors at their chosen depth, which smoothed the data and removed divergences. Pollard et al. (1995), using data from a repeated survey later in the *Discovery* Sterna cruise, have compared ADCP current profiles from the same position 3.4 inertial periods apart. In that example they showed that inertial oscillations were confined to the top 120 m and that the geostrophic current profile was altered by less than 0.05 m s^{-1}, while the surface ageostrophic currents changed by nearly 0.3 m s^{-1}. The only test of whether ADCP velocities are nearly geostrophic below the mixed layer that we can apply is to compare subjectively the ADCP and geostrophic shears (Fig. 3). The profiles shown span the eddy centered at 55.2°S (Fig. 2). Cross-track ADCP velocities at 196 m reversed from west to east through the eddy (Fig. 4), and both ADCP and geostrophic shears also reverse (Fig. 3).

Various criteria have been tested to achieve the best fit between geostrophic shear and ADCP profiles, matching at a depth or over a depth range from 16 to 440 m. The change in rms fit using this range of criteria varied by less than 3 cm s^{-1}. We have therefore chosen a simple match at 196 m, as this has the advantage of

Unauthenticated | Downloaded 01/22/22 03:01 AM UTC

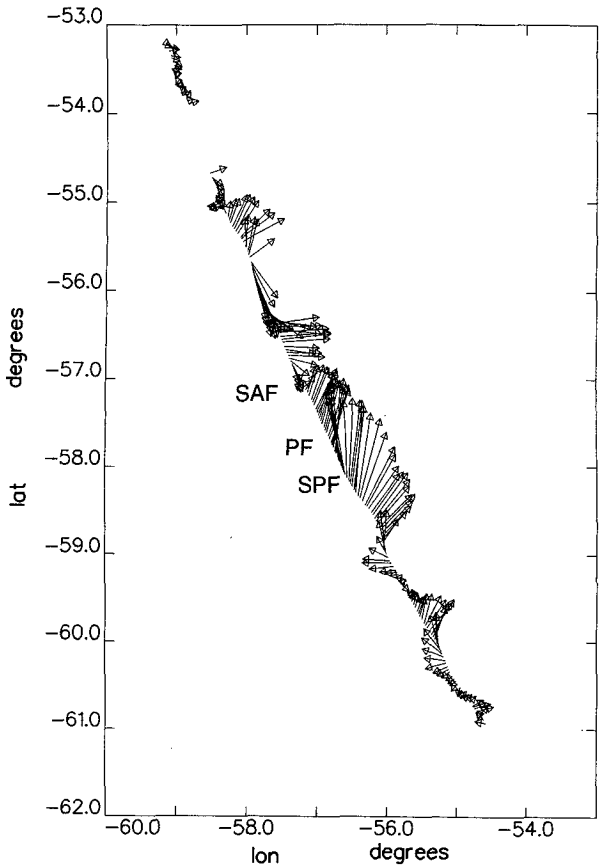

FIG. 4. ADCP current vectors at a depth of 196 m plotted along the cruise track. Each vector is an average over 12 km and a vector is plotted every 4 km. The estimated error in each vector is 0.05 m s^{-1} (Griffiths 1994). Approximate frontal positions are marked (see Fig. 2 for abbreviations).

enabling SeaSoar data south of 59°S to be used (Fig. 2). Over most of the depth range, the difference between the geostrophic and ADCP profiles is less than 0.05 m s^{-1} (Fig. 3). The only exceptions are very near the surface, where large ADCP shears are most probably inertial or Ekman in origin, and at the bottom of some ADCP profiles, where there are too few data to form a reliable time average. After comparing the profiles for the whole section (of which only a small part can be shown in Fig. 3), we estimate that the error in surface geostrophic velocities is typically 0.1 m s^{-1}, in some cases larger. In the high current regime in Drake Passage, derived surface geostrophic velocities are typically 0.5 m s^{-1} (Fig. 5). Thus, the method has a good signal to noise ratio where there are major ocean currents.

Tidal currents cannot be eliminated. The Cartwright and Ray (1990) tidal model is used to remove tidal heights from the altimetry, but it is not possible to estimate the tidal currents from such a model. In some instances, for instance between 55.6° and 55.8°S, there are current structures in the in situ dataset that we believe to be in error. Because corresponding features do not occur in the altimetric dataset, these structures propagate into all passes. Examining the in situ data in detail reveals that to remove these structures would involve moving the geostrophic shear relative to the ADCP shear by a much larger offset than can be justified from the data. We believe that this offset is the result of tidal currents present in the ADCP data.

b. ERS-1 data

There are two common sets of *ERS-1* data in usage: the IGDR's (Interim Geophysical Data Records) distributed by NOAA and the off-line OPR product from the French PAF (Processing and Archiving Facility). The off-line altimeter product (version 3) was used in this study. The 35-day repeat mission of *ERS-1* lasted from April 1992 until December 1993, so a maximum of 17 passes should be available. In practice, it was found that useful amounts of data could be recovered from 11 passes. The passes used in this study were on days 139, 174, 209, 244, 279, 314 (which is the closest pass to the *Discovery* data), and 349 of 1992 and days 18, 158, 193, and 263 of 1993. The orbit used was that issued by ESA with the OPR data, and the corrections included with the product were used with the exception of the tidal correction. The Schwiderski tide distributed by ESA was replaced by the Cartwright and Ray tide (Cartwright and Ray 1990). No corrections were made for sea-state bias or the inverted barometer.

The tracks involved here are very short, so it is difficult to perform any empirical orbit correction on them. Instead, much longer tracks covering the whole Southern Hemisphere (from the equator downcrossing in the Indian Ocean to the upcrossing in the Pacific) were extracted. The data were collocated in time to 1-s values from the downcrossing of the equator. Any point without data on each pass was excluded from the analysis, as were any points over ice. A mean sea surface was then calculated and subtracted from each pass. A once per revolution sine curve was fitted to the residuals. This correction was then subtracted from the shorter tracks across Drake Passage. By using a much longer sequence of data for the extraction of the orbit, any influence of currents in Drake Passage on the orbit correction is minimized.

Once the altimeter data had been corrected, they were interpolated to a 0.06° latitude grid using cubic spline interpolation. The sea surface heights produced are plotted in Fig. 6. This shows the magnitude of the gravity signal. A number of points are worthy of note. The first is the gravity signal from the Burdwood Bank, and the second is the difference in variability between the deep water channel and the shallow water over the bank. The feature at 57.1° will be referred to later. This height signal was then numerically differentiated using a central difference formula

Unauthenticated | Downloaded 01/22/22 03:01 AM UTC

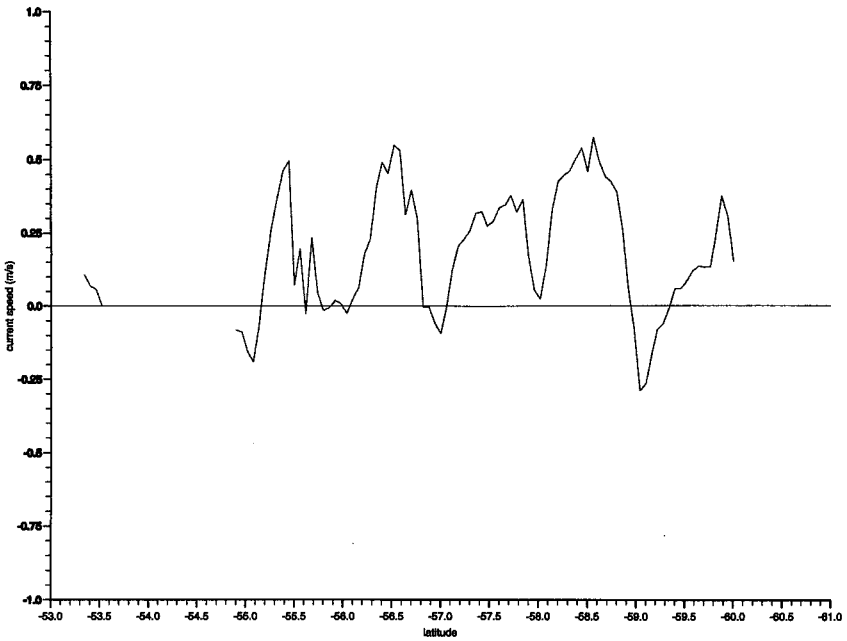

FIG. 5. Cross-track surface geostrophic velocity as a function of latitude derived from combination of ADCP and SeaSoar data. Typical values are 50 cm s^{-1}, while our estimate of the errors in matching ADCP and SeaSoar profiles is typically 10 cm s^{-1}.

$$\dot{h}_i = \frac{(h_{i+1} - h_{i-1})}{d},$$

where d is twice the distance between data points and is taken to be 14 km here.

The data were then smoothed with a three-point running average. This reduces the high-frequency noise on the altimeter. It could be argued that the data should be smoothed before the derivatives were taken rather than the other way around. In practice, the difference in the results is small.

Once we have the smoothed estimates of surface slope, these can be converted to geostrophic currents normal to the satellite track

$$v_t = \frac{g}{f}\frac{\partial h}{\partial x}.$$

However these are not "true" currents because the slopes still contain the gravity signal. In a standard altimeter analysis the mean of all the tracks would be set to zero. Here, however, we will use the track on day 314 as a reference. The currents on this pass are therefore set to zero and the currents on the other passes are calculated relative to day 314. The resulting geostrophic currents are shown in Fig. 7.

We have not applied an inverse barometer correction to the altimeter data used above. Reproducing the calculations including such a correction resulted in no appreciable difference to the results. This is not surprising since the inverse barometer correction varies on the large scale associated with atmospheric pressure variations. As pointed out above, large-scale corrections will be nearly constant across the passage and, when differentiated, the correction will disappear. Similarly, we have not applied a sea state (or EM) bias correction to the data.

c. *Combining the data*

We now have two datasets. From the *Discovery* hydrographic data we have geostrophic surface currents for days 315 and 316, while from *ERS-1* we have currents every 35 days relative to day 314. If we make the assumption that there is no change in current between day 314 and day 316, we can combine these two sets very simply. Following Eqs. (5) and (9), we add the relative current from each *ERS-1* pass to the *Discovery* data to obtain the absolute currents at the time of each satellite overpass. The resulting currents are shown in Fig. 8.

Figure 9 shows the mean surface current and the standard deviation calculated about that mean. Note that the mean current is highly structured, whereas the standard deviation is flat across the passage. One implication of this is that, if we had used "classical" techniques to calculate the mesoscale variability from the radar altimeter data, the result would have failed to show any of the structure visible in the currents shown in Fig. 8.

Looking at the data in more detail, it is immediately clear that the ACC in this region consists of two

Unauthenticated | Downloaded 01/22/22 03:01 AM UTC

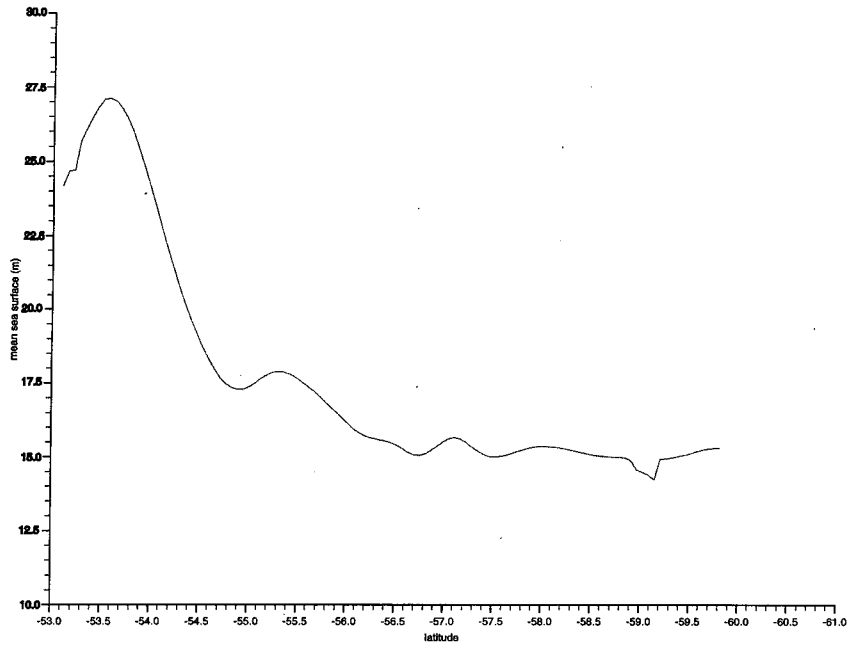

FIG. 6. The sea surface elevation across the section as measured by *ERS-1*. The signal is dominated by the gravity signal. Note the very large signal from the Burdwood Bank (at 53.5°S) and the local maximum at 57.2°S implying the existence of a topographic feature.

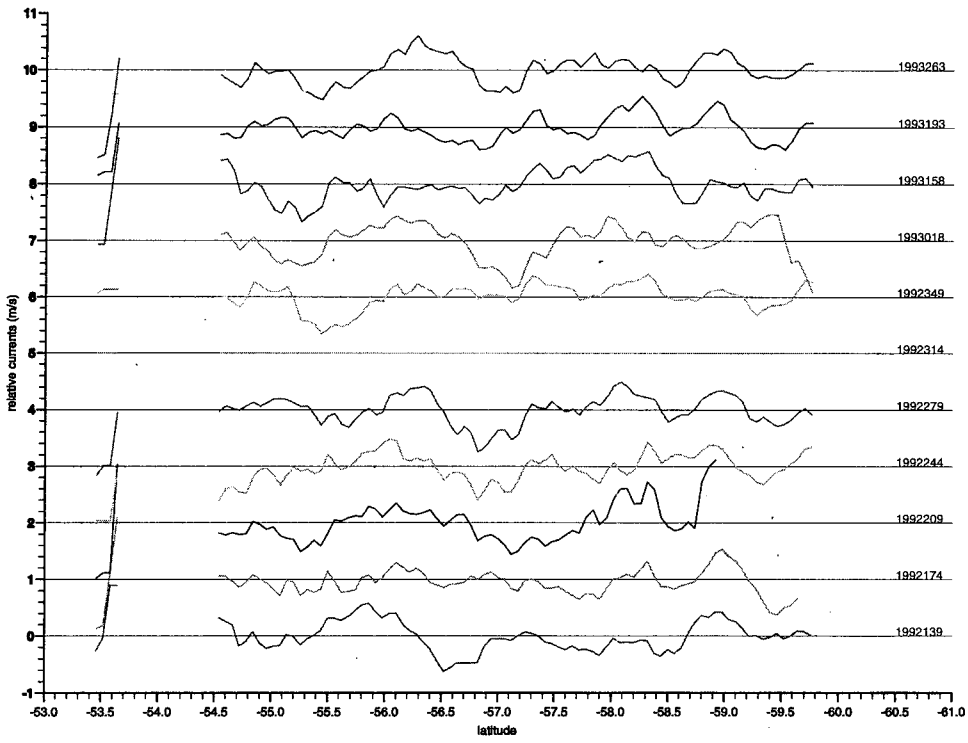

FIG. 7. Cross-track surface geostrophic velocities from *ERS-1* calculated relative to the pass on day 314. (Each pass has been offset by 1 m s^{-1}) The labels give the dates of the satellite passes.

Unauthenticated | Downloaded 01/22/22 03:01 AM UTC

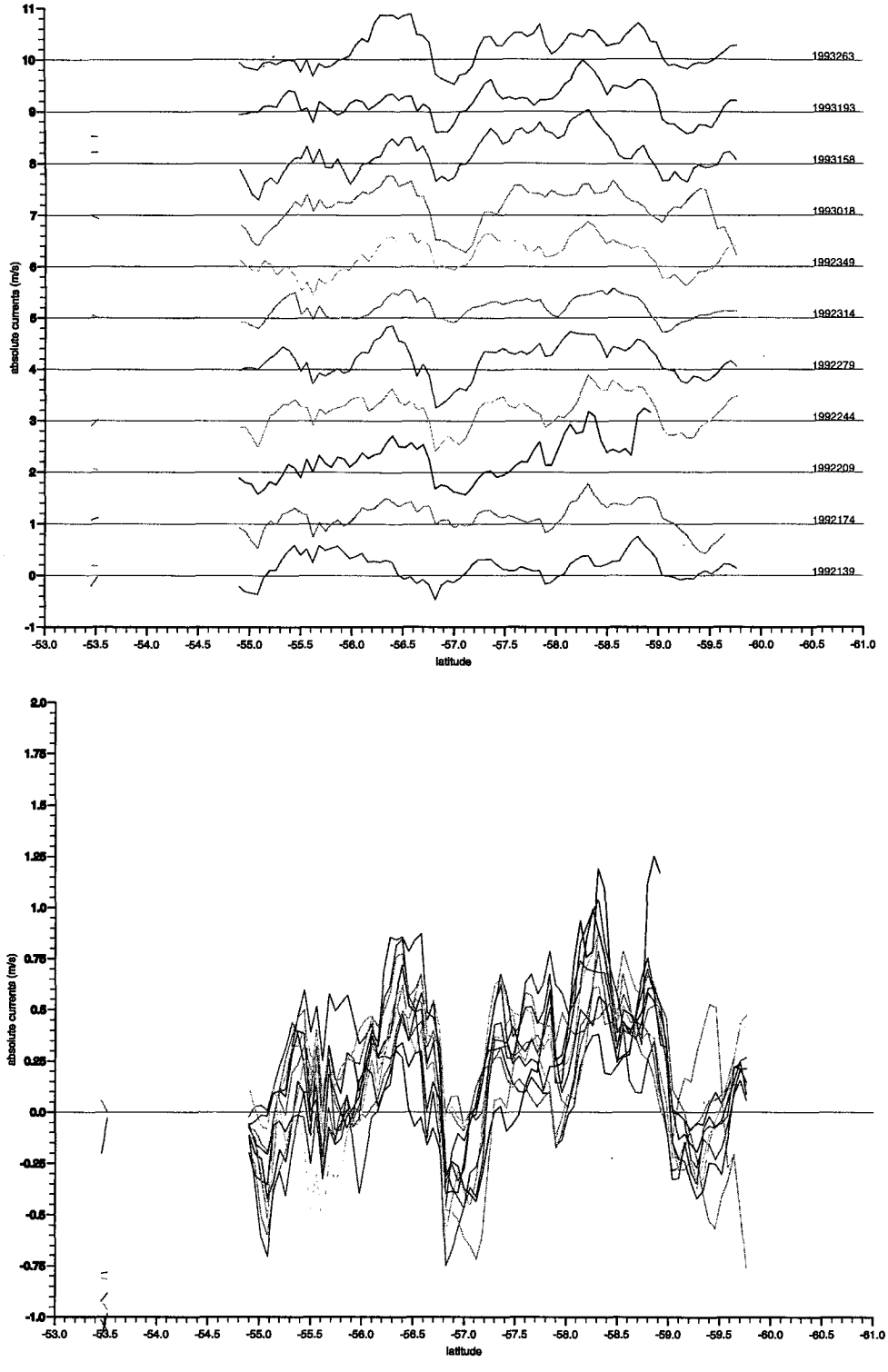

FIG. 8. Cross-track surface geostrophic velocities (a) offset and (b) overlaid for each of the *ERS-1* 35-day repeat cycles matched to the ship-derived values (Fig. 5) for day 314.

Unauthenticated | Downloaded 01/22/22 03:01 AM UTC

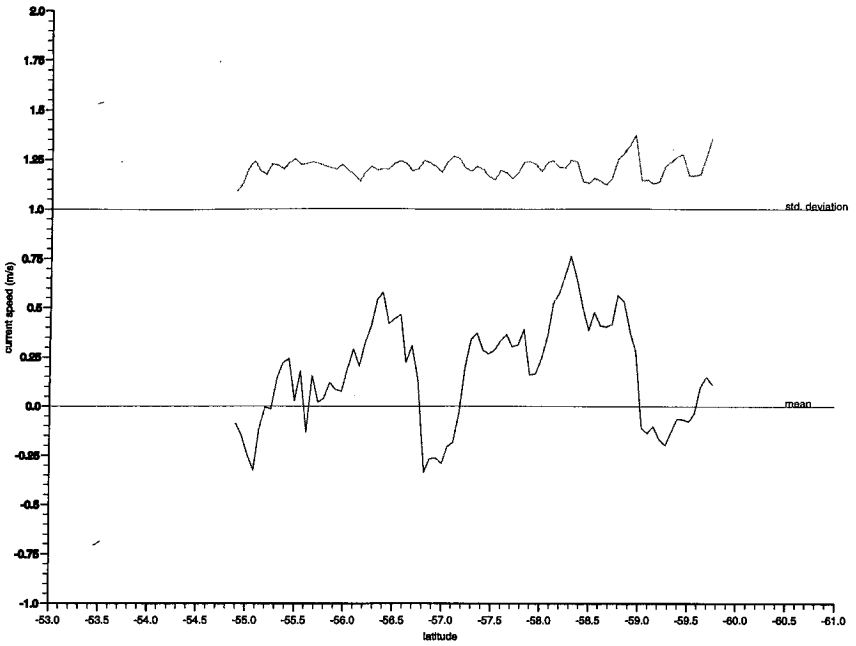

FIG. 9. The mean and standard deviation of cross-track surface geostrophic velocities (the standard deviation has been offset by 1 m s^{-1}).

streams, corresponding broadly to the Subantarctic and Polar Fronts respectively north and south of 57°S. The Polar Front gives rise to a broader and, on average, a stronger current. On several passes the Polar Front appears itself to be split into two parts, north and south of 58°S, which would correspond to the Polar and Southern Polar Fronts proposed by Read et al. (1995). Of interest is the region around 57°S in between the strong eastward flow associated with the Subantarctic and Polar Fronts. Here the flow is either very small or is to the west. Although the width and strength of this westward flow varies, the position of its northern boundary is remarkably consistent at 56.8°S. There are other regions of zero or westward flow too, between 55.0° and 55.1°S and south of 59°S. It is difficult to explain the persistence of these flows in terms of propagating eddies. This problem will be discussed further below.

d. *Comparison with in situ measurements*

Having produced a new dataset such as this, it is important to validate it. Unfortunately there are no independent data taken during the period of our measurements. A series of current meters were deployed in Drake Passage during the ISOS experiment in 1977 (Wright 1981). These meters were much farther to the west than our line (near 64°W), and the shallowest meter was at a depth of 360 m. The mean current in approximately the same direction as ours (062°T) was 0.23 m s^{-1} compared with 0.35 from our method. The standard deviation is 0.14 m s^{-1} compared to our mean standard deviation of 0.33 m s^{-1}. Given the difference in depth of the two measurements and that ours is an estimate of the geostrophic current, this comparison is not unreasonable.

e. *Comparison with a model*

The strength of the currents can be verified to some extent by comparison with historical current meter data. It is more difficult to show that the pattern of currents is correct. The general shape of the currents in Drake Passage with the two eastward flowing strong currents corresponding to the Polar and Subantarctic Fronts is well known (see, e.g., Nowlin et al. 1977; Peterson et al. 1982). What needs to be explained is the westward flowing component between the two fronts and its invariant position in space for the duration of the measurements.

There is evidence for a small westward flowing surface current in Nowlin et al. (1977) just south of 58°S; however, the magnitude of this current is less than 0.05 m s^{-1}. All the large westward currents in our data come from the combined data, and we need to verify that they have not been caused by the altimeter processing, while noting that the density data (Fig. 2) clearly confirm that on day 316 there was westward geostrophic flow at the surface relative to 400 m. In the absence of any further in situ data we turn to the one-quarter degree resolution Parallel Ocean Climate Model (POCM) (Semtner and Chervin 1992). The run we have used covers about

Unauthenticated | Downloaded 01/22/22 03:01 AM UTC

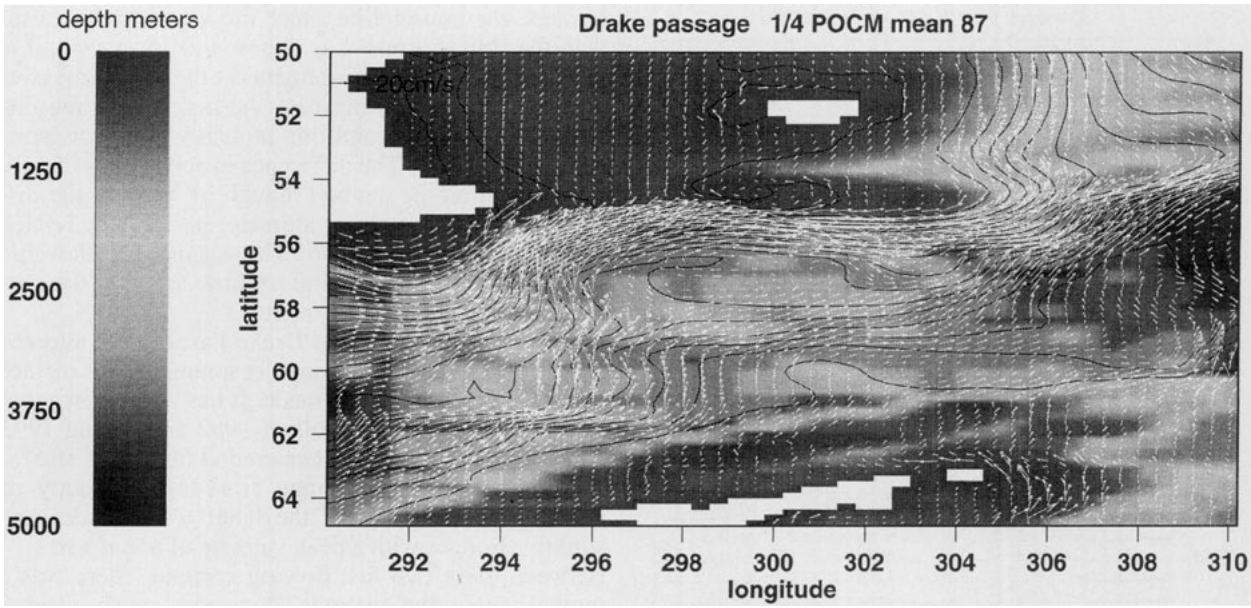

FIG. 10. Mean flow through the Drake Passage for 1987 from the Parallel Ocean Climate Model. The shading shows the bottom topography, the contours, the mean sea surface height, and the arrows show the current in the top layer (12.5 m) of the model.

four years (April 1986–89), with the wind stress for this period from the ECMWF. The model resolution at a latitude of 33° is one-third degree and at 68° the resolution is one-fifth degree, therefore averaging to one-quarter degree spatial resolution. Additional changes from the one-half degree model run (Semtner and Chervin 1992) include a free surface using the formulation of Killworth et al. (1991) and heat flux and salt flux (Haney 1971) restoring to seasonal cycles of Levitus data only in the uppermost levels. Subsurface restoring of temperature and salinity only occurs north of 58°N and south of 68°S. The model run was initialized using the 33-year spinup of the half-degree run, starting with January 1986 ECMWF winds. The free surface formulation allows the model to include unsmoothed topography. Since the model is attempting to simulate different years from our data, we would not expect exact agreement even if the model were perfect. Figure 10 shows the topography of the region with the black contour lines representing the 1987 mean surface height field from the model overlaid with the velocity vectors for the top level of the model (12.5 m). Consistent with the in situ data, the model simulation produces two strong eastward flowing currents at 59°W, one centered at 55.5°S (1.00–1.20 m s^{-1}) and the other centered at 58.5°S (0.50 m s^{-1}). Between these two regions is a weaker flow region that shows some recirculation between 62° and 58°W (0.05–0.10 m s^{-1}). The figure suggests that the Antarctic Circumpolar Current follows the deeper channels in this area, splitting at 63°W to flow around a slightly elevated feature (3575 m with the channels at 4125–4600 m). Zonal geostrophic velocities were computed from the model monthly sea surface height fields for the complete simulation to compare to the cross-ship-track velocities calculated from altimeter and in situ data (Fig. 11). The figure clearly shows that the northern branch of the current is very permanent, varying little over the almost four years of the simulation. The weaker southern branch shows some variation over the year, with a narrower width in the austral summer (Nov–Feb) and broader stream in the austral winter (Jun–Aug). EOF calculation performed on the 1987–88 wind stress field shows that the first two modes explain about 95% of the variability (81% for the first mode and 14% for the second mode). No clear seasonal cycle is seen from the EOF calculation; therefore, the model simulation would suggest that the flow is mostly topographically driven. If the intermittent westward flow comes from instabilities in the current (see Peterson et al. 1982), then the position of the fronts would move north and south as these eddies are shed. The only explanation is that the westward currents do not come from rings moving with the ACC but from features that are being steered by the topography. The model clearly shows this behavior. We believe that the reason the model results appear to be displaced relative to the data is due to errors in the model's bottom topography, as shown in Fig. 10.

Unfortunately we cannot confirm the association of the currents with the topography, and the error in the model topography, from in situ data as the deep echo sounder did not work well on the cruise. However, the sea surface elevation from the altimeter (Fig. 6) clearly

Unauthenticated | Downloaded 01/22/22 03:01 AM UTC

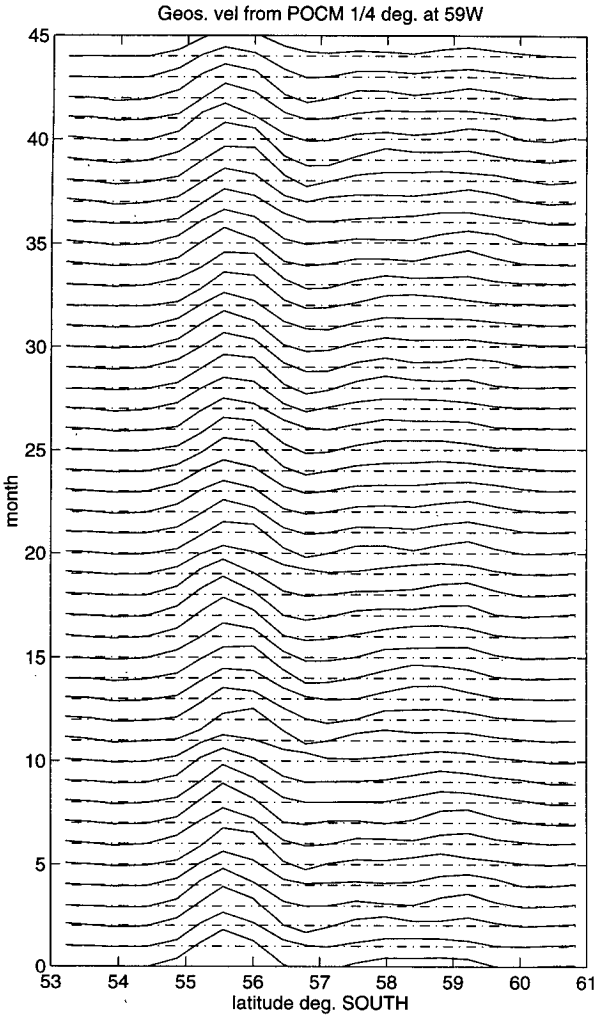

FIG. 11. Zonal surface geostrophic velocities at 59°E from the POCM.

shows a local maximum coincident with the westward flow, implying that there is a topographic feature there.

5. Conclusions

We have shown by using a combination of ship measurements of density and current and satellite altimeter measurements that it is possible to produce absolute surface currents from altimetry. This enables the uncertainty about the earth's gravity field to be overcome. The method has been applied here to a section across Drake Passage. However, the technique is general and could be applied in other regions. The only requirements are that the ship follows the altimeter track and measures both density and current profiles. One limitation not discussed is the time difference between the altimeter pass and the ship measurements. In our case it was not possible to have the ship measurements at exactly the same time as the altimeter pass. In fact, because the subsatellite point moves so much faster than the ship (7 km s^{-1} as opposed to 15 m s^{-1}), it is impossible to take measurements at the same time over a useful distance. In our case the maximum time difference is two days and this probably does not introduce a large error. The difference in speed does impose a limitation on the method though by limiting the distance over which a single altimeter pass can be related to a hydrographic section. The maximum allowable time difference will depend on how variable the currents are in the region of interest.

Applying the method to Drake Passage has allowed a series of high-resolution measurements of surface geostrophic current to be made. It has been shown that the ACC in the second half of 1992 and during 1993 consisted of two streams centered at 56.5° and 58.5°S. The former had an average cross-track velocity of about 0.75 m s^{-1}, while the latter was broader and slightly stronger with a peak velocity of about 1 m s^{-1}. Between these two fast flowing currents, there was a region where the average flow was much weaker (about 0.25 m s^{-1}) to the west. All these features are remarkably consistent in position, although it should be noted that within this general shape the structure is quite variable. Similar current structures are seen in results from the Parallel Ocean Climate Model. Again the features remain fixed in position. For the model the correlation of the flow with the bathymetry is clear. We suggest that we are seeing a similar phenomenon in the data and that the positions of the currents across the section are strongly related to the bottom topography. The displacement of the features in the data and the model is due to errors in the model bathymetry.

Acknowledgments. We would like to thank ESA for providing us with the *ERS-1* altimeter data.

REFERENCES

Cartwright, D. E., and R. D. Ray, 1990: Oceanic tides from GEOSAT altimetry. *J. Geophys. Res.*, **95,** 3069–3090.

Gleason, D. M., 1991: Obtaining Earth surface gravity disturbances from a GPS-based 'high–low' satellite-to-satellite tracking experiment. *Geophys. J. Int.*, **107**(1), 13–23.

Glenn, S. M., D. L. Porter, and A. R. Robinson, 1991: A synthetic geoid validation of Geosat mesoscale dynamic topography in the Gulf Stream region. *J. Geophys. Res.*, **96**(C4), 7145–7166.

Griffiths, G., 1994: Using 3D GPS heading for improving underway Acoustic Doppler Current Profiler data. *J. Atmos. Oceanic Technol.*, **11,** 1135–1143.

Haney, R. L., 1971: Surface thermal boundary condition for ocean circulation models. *J. Phys. Oceanogr.*, **1,** 241–248.

Jekeli, C., and T. N. Upadhyay, 1990: Gravity estimation from STAGE, a satellite-to-satellite tracking mission. *J. Geophys. Res.*, **95**(B7), 10 973–10 985.

Kelly, K. A., and S. T. Gille, 1990: Gulf Stream surface transport and statistics at 69°W from the Geosat altimeter. *J. Geophys. Res.*, **95**(C3), 3149–3161.

Killworth, P. D., D. Stainforth, D. J. Webb, and S. M. Paterson, 1991: The development of a free-surface Bryan–Cox–Semtner ocean model. *J. Phys. Oceanogr.*, **21,** 1333–1348.

King, B. A., and E. B. Cooper, 1993: Comparison of ship's heading determined from an array of GPS antennas with heading from

Unauthenticated | Downloaded 01/22/22 03:01 AM UTC

conventional gyrocompass measurements. *Deep-Sea Res.*, **40,** 2207–2216.

Lambeck, K., 1990: Aristoteles: An ESA mission to study the Earth's gravity field. *ESA Journal,* **14**(1), 1–21.

Mitchell, J. L., J. M. Dastugue, W. J. Teague, and Z. R. Hallock, 1990: The estimation of geoid profiles in the northwest Atlantic from simultaneous satellite altimetry and airborne expendable bathythermograph sections. *J. Geophys. Res.,* **95**(C10), 17 965–17 977.

Nowlin, W. D. J., T. Whitworth, and R. D. Pillsbury, 1977: Structure and transport of the Antarctic Circumpolar Current at Drake Passage from short-term measurements. *J. Phys. Oceanogr.,* **7,** 788–810.

Ozimek, K., P. Flament, E. Firing, J. Read, R. Pollard, and J. Luyten, 1993: Shipboard acoustic Doppler current profiler data from the Agulhas Current and Retroflection region. University of Hawaii SOEST Tech. Rep. 93-04, 85 pp. [Available from University of Hawaii at Manoa, 1000 Pope Road, Honolulu, HI 96822.]

Peterson, R. G., W. D. J. Nowlin, and T. Whitworth, 1982: Generation and evolution of a cyclonic ring at Drake Passage in early 1979. *J. Phys. Oceanogr.,* **12,** 712–719.

Pollard, R. T., 1986: Frontal surveys with a towed profiling conductivity/temperature/depth measurement package (SeaSoar). *Nature,* **323,** 433–435.

——, and J. Read, 1989: A method of calibrating ship-mounted acoustic doppler profilers and the limitations of gyro compasses. *J. Atmos. Oceanic Technol.,* **6,** 859–865.

——, and L. A. Regier, 1992: Vorticity and vertical circulation at an ocean front. *J. Phys. Oceanogr.,* **22,** 609–625.

——, J. F. Read, J. Smithers, and M. W. Stirling, 1987: SeaSoar sections from the Antarctic Circumpolar Current at 52°S, 32°E to the Subtropical Front at 37°S, 52°E. Institute of Oceanographic Sciences Deacon Laboratory, Southampton Oceanography Centre, Southampton, U.K., Rep. 244, 55 pp.

——, ——, J. T. Allen, G. Griffiths, and A. I. Morrison, 1995: On the physical structure of a front in the Bellingshausen Sea. *Deep-Sea Res.,* **42**(415), 955–982.

Read, J. F., J. T. Allen, P. Machin, G. W. J. Miller, A. I. Morrison, R. T. Pollard, and P. G. Taylor, 1993: SeaSoar data collected on RRS Discovery Cruise 198 (Sterna) across Drake Passage and in the Bellingshausen Sea. Internal Document No 320, Institute of Oceanographic Sciences Deacon Laboratory, Southampton Oceanography Centre, Southampton, U.K., 57 pp.

——, R. T. Pollard, A. I. Morrison, and C. Symon, 1995: On the southerly extent of the Antarctic Circumpolar Current in the southeast Pacific. *Deep-Sea Res.,* **42,** 933–954.

Semtner, A. J., and R. M. Chervin, 1992: Ocean general circulation from a global eddy-resolving model. *J. Geophys. Res.,* **97**(C4), 5493–5550.

Turner, D. R., 1993: BOFS 'Sterna 92' Cruise Report: Discovery 198 11/11/92–17/12/92. Plymouth Marine Laboratory, Plymouth, U.K., 85 pp.

Wright, D. G., 1981: Baroclinic instability in Drake Passage. *J. Phys. Oceanogr.,* **11,** 231–246.

Unauthenticated | Downloaded 01/22/22 03:01 AM UTC